Resilience assessment of high damping rubber bearings in beyond-design conditions

“Beyond design” modeling of HDRB seismic isolators under cyclic loading

M. Domaneschi[1], L. Martinelli [2], G.P. Cimellaro [3]

[1] *Politecnico di Torino, Department of Structural, Geotechnical and Building Engineering, Turin IT, Email:* marco.domaneschi@polito.it [2] *Politecnico di Milano, Department of Civil and Environmental Engineering, Milan IT, Email:* luca.martinelli@polimi.it [3] *Politecnico di Torino, Department of Structural, Geotechnical and Building Engineering IT, Email:* gianpaolo.cimellaro@polito.it

Abstract

Passive isolation systems are an established solution for the design of civil engineering structures that are required to provide superior performances in the case of a seismic event. Although their application to the seismic protection of bridges is currently limited, isolation systems are likely to become more widespread in the design of strategic infrastructures and facilities. In this work numerical investigations on the ultimate limit state conditions of filled high damping rubber bearings under cyclic shear loading are presented, focusing on the influence of the axial load with respect to the device.

1. Introduction

In the recent past, passive isolation systems have been largely used as a valuable earthquake-resistant strategy in the design of civil engineering structures, particularly with reference to the large class of ordinary buildings. Indeed, passive, anti-seismic, systems have already been used to protect more than 23000 structures such as bridges and buildings, both existing and of new construction, in more than 30 countries, although their introduction for the seismic protection of strategic structures, such as bridges, is not as widespread as their use for buildings.

Nevertheless, seismic isolation systems are likely to become an established highly reliable solution in the design of special structures and facilities for which superior performances are needed against, and functionality after a seismic event is of utmost importance (De Grandis et al 2009, Perotti et al 2013). Indeed, transportation network and infrastructures are expected to remain in service also after disruptive events for emergency activities.

The anticipated better performance of isolated structures, when compared to traditional ones, consists in reducing the values of the seismic acceleration transmitted to the part of the structure above the isolation plane (the superstructure). This attenuation is obtained at the price of larger relative displacements between the superstructure and the under-structure.

Where isolation devices are installed they are likely to become the most critical components in a seismic assessment. Thus, all factors affecting the devices performance have to be carefully considered. A reliable and close to reality evaluation of the constitutive behaviour, up to the device limit state, need to be fully addressed.

Failure of isolators is obviously related to “be-yond design” loading conditions, i.e. extreme loading in case of very strong seismic events which lead to amplified multi-directional loading paths in the horizontal plane and to variable axial loading. Such extreme circumstances cannot be excluded during the structure’s life, and their study requires reliable and validated constitutive models of the isolator de-vices.

Reliable models of the behaviour of seismic isolation devices, and the evaluation of their performance, has been successfully accomplished with selected constitutive material laws by FE

modeling for moderate, to large, shear strain values. For very large values of the shear strain cyclic constitutive models are however still lacking (Domaneschi et al 2015).
This research is devoted to the implementation and validation of special hyperelastic-dissipative material models, which are promising of a good phenomenological interpretation of the cyclic physical behaviour of the isolators when subjected to very large shear strains and axial loads. The ultimate goal is the implementation in finite element models of large bridge structures.
Furthermore, since as it has been pointed out (e.g. by Warn and Whittaker 2008), in application of isolation devices to bridges, a variation of the vertical load carried by the devices has to be expected as well. Therefore, the isolators models are tested in the case of different values of the axial force and the influence of the device shape is highlighted.

2. Physical and numerical models of the isolator device

In the class of isolator devices a basic distinction is based on shape, materials and dimensions. The most commonly adopted solution in the world is rep-resented by the steel-laminated rubber bearings, especially high damping rubber bearings (HDRB) and the lead rubber bearings (LRB) for which the largest experience has been gathered and detailed literature is provided (see e.g. Basu et al. 2014). A schematic geometry of an elastomeric isolator is depicted in Fig. 1 with a physical example.
The relevant role fulfilled by seismic isolation de-vices in seismic engineering is due to the fact that these devices are able to ensure large deformations in the horizontal plane in case of a seismic event and provide high stiffness in the vertical direction to sustain gravitational loads. These effects are obtained through the low compressibility of rubber and the introduction of thin reinforcing steel plates. Therefore, among different technologies the steel-laminated rubber bearings, especially the high damping rubber bearings (HDRB) and the lead rubber bearings (LRB), represent the most commonly adopted solution in the world (Basu et al 2014).
The failure of the isolators, in the case of very strong seismic events, is related to extreme loading conditions, that induce amplified multi-directional loading paths in the horizontal plane and a highly variable axial loading.
To study the device behaviour under these circumstances FE models employing an overlapping discretization are a promising approach, when supported by experimental data. This technique is based on the concept that the material behaviour can be split in-to a number of parallel fractions, each one with conventional mechanical properties and hence available constitutive laws (hyper-elastic, elastic-plastic and viscoelastic). The global behaviour is achieved by a suitable superposition of simple constitutive models and adequate material parameters. In this way a robust FE model for HDRB devices can be developed (Milani & Milani 20112, Gracia et al 2010), on the basis of overlapped constitutive laws and fitting of standard laboratory test data.
The translation of this concept in FE analyses re-quires the generation of a numerical model with several identical overlaid meshes, sharing the same nodes, each one presenting a different constitutive model.
For these devices, an adequate mathematical model should not only reproduce the basic elastic behaviour of the rubber, but has also to account for dissipative properties within a large deformation range. Damping factors for a HDRB ranges from 10% to 15%, while shear modulus (G) lies in the 0.8-1.4 MPa range (Perotti et al 2013).
Furthermore, the extreme value of the axial load can be achieved at or near the one of the relative displacement, so that the dimension of the device become important. To study the effect of this parameter, extreme possible geometries of the isolation device have been selected in the simulation of the global cyclic behaviour in isolators undergoing variable seismic and axial loads.

Three FE models of a circular HDRB (Fig. 2) have been developed within the MARC® FE code, according to the geometrical properties listen in Tables 1-3. The characteristics of the first HDRB de-vice closely reproduce the prototypes designed and tested for the ELSY reactor within SILER project (2013).

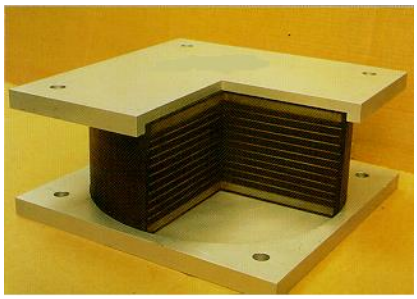

Figure 1. Physical example of the isolator device.

Table 1. Properties of the first HDRB device modelled.

Diameter	1350 mm
Total rubber thickness	256 mm
Thickness of each rubber layer	16 mm
Steel layers	15
Shape factor	19.7
Rubber lateral cover thickness	25 mm
Rubber shear modulus	1.4 MPa
Horizontal stiffness (100%)	7.82 kN/mm
Vertical stiffness	5792 kN/mm

Table 2. Properties of the device 601 in (Nagarajaiah & Ferrell 1999).

Diameter	10 in
Total rubber thickness	2.00 in
Thickness of each rubber layer	0.25 in
Rubber layers	8
Rubber shear modulus	1.4 MPa

Table 3. Properties of device 302 in (Nagarajaiah & Ferrell 1999).

Diameter	5 in
Total rubber thickness	2.00 in
Thickness of each rubber layer	0.25 in
Rubber layers	8
Rubber shear modulus	1.4 MPa

The other two are inspired by the geometry of bearing 601 and 302 in (Nagarajaiah & Ferrell 1999).

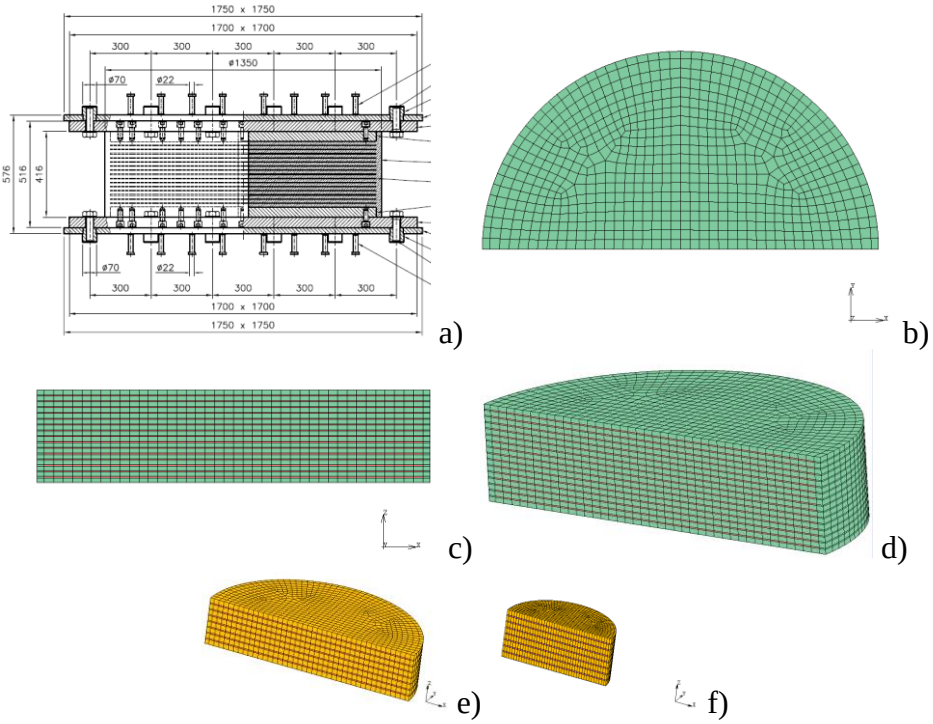

Figure 2. Design table (a) and finite element 3D mesh of the first (SILER) device (b-d). FE mesh of the devices 601 and 302 (e-f) respectively in (Nagarajaiah & Ferrell 1999).

The finite element mesh for the first (SILER) de-vice has been prepared considering symmetry of geometry and boundary conditions. In the end, it consists in about 35000 isoparametric hexahedral solid elements and 25000 nodes.

According to the overlapping simulation approach, rubber layers are composed by two overlap-ping meshes: to one is assigned an hyperelastic behaviour, to the other an elastic-plastic one to ensure dissipation will be achieved.

The models from (Nagarajaiah & Ferrell 1999) have a mesh similar to the first one. It is obtained by an operation of geometric scaling without changing the number of elements or of nodes for each number of constitutive rubber-steel layers.

For all FE models, the hyperelastic behaviour is simulated according to a three-constants Mooney-Rivlin model (Yeoh model), usually implemented in common commercial FE codes. The material parameters are assumed to be equal to the ones derived in (Gracia et al 2010), whose assessment is based on the execution of laboratory tests on HDRB under cyclic relative displacements and constant axial force, carried on up to the specimen failure. Their corresponding values are listed in Table 4.

Table 4. Value of the constants in the Mooney-Rivlin material model.

C10	4.989×10^{-1}
C20	3.47×10^{-2}
C30	2.28×10^{-3}

The values in Table 4 are also in agreement with the those independently identified in (Bianchi et al 2011a, 2011b) for similar conditions.

The elastic-plastic behaviour assigned to the second mesh within the par of the isolator model occupied by the volume of the elastomeric component, is derived from the von Mises' theory. The preliminary fitting of the experimental outcomes have been processed assuming a perfectly elastic-plastic behaviour defined by values in Table 5.

Table 5. Material parameters for the elastic-plastic material model.

Young modulus E (MPa)	11.28
Poisson's ratio ν	0.00
yielding stress f_y (MPa)	0.49

Finally, a non-linear elastic perfectly plastic material (Young modulus 210000 MPa, Poisson's ratio 0.3, yielding 300 MPa) has been assigned to the steel layers.
The boundary conditions on the FE model consist in fixed displacements at the device base, imposed uniaxial horizontal displacement (100% of rubber thickness) at the upper isolator surface, constant vertical load at the top. Fig. 3 depicts the comparison between laboratory data and FE model simulation.

3. Numerical results

The loading conditions herein presented aim to analyze the influence of the axial force on the hysteresis cycles. Thus, subsequently to the identification of the material parameters on the base of an experimental uniaxial horizontal test, different vertical loads have been applied on the finite element model of the device. Furthermore, the limit condition at failure (delamination mode), as reproduced in laboratory tests, has been simulated by FE analyses in or-der to identify the corresponding stress state. This development are based on numerical analysis on FE models of the device carried out within the MARC® FE code.

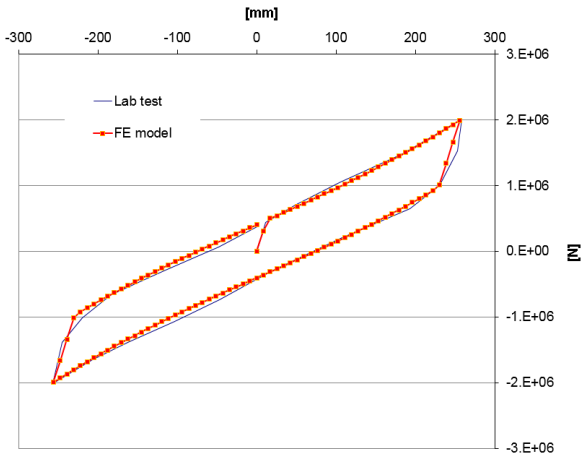

Figure 3. Comparison between laboratory tests hysteresis cycle (100% - 256 mm - horizontal uniaxial displacement) at constant axial load (8075 kN, halved due to symmetry) and FE simulation. SILER isolator.

Initial validation of the adopted material values has been performed with reference to data from the physical testing of the isolator (SILER 2013). The boundary conditions in the FE model, which have been retained with the exception of the value of the axial load, consist in fixed displacements at the de-vice base, imposed uniaxial horizontal displacement (100% of rubber thickness) at the upper isolator sur-face, constant vertical load at the top. Fig. 3 depicts the comparison between the FE model simulation and laboratory data.
The FE model, validated by the good matching with experimental data reported in in Fig. 3, has been exploited for evaluating the influence of axial load variations on the performance of the device. The analyses take into account mechanical and geo-metric non-linearities in order to study possible be-yond design conditions.

At first, the same loading path of Fig. 3 has been reproduced with double (16500 kN) and triple axial force (24800 kN). Furthermore, zero axial force is al-so investigated. As it can be inferred from Fig. 4a, that depicts for these values of the axial load the isolator cyclic response up to 100% of shear deformation in the rubber layers, there is no influence of this static parameters, at least at these deformation values.
The same axial forces have been used to study the device with monotonically increasing horizontal imposed displacements corresponding to 300% and 600% of shear strain. Figures 4b and 4c report the loading paths in terms of force–displacements at 300% and 600% of shear strain, respectively.
All the responses appear substantially equivalent, although for the horizontal displacements at 600% shear strain minor differences among the curves can be detected. For the same 600% condition the analysis has not been completed due to excessive deformation in some finite elements.

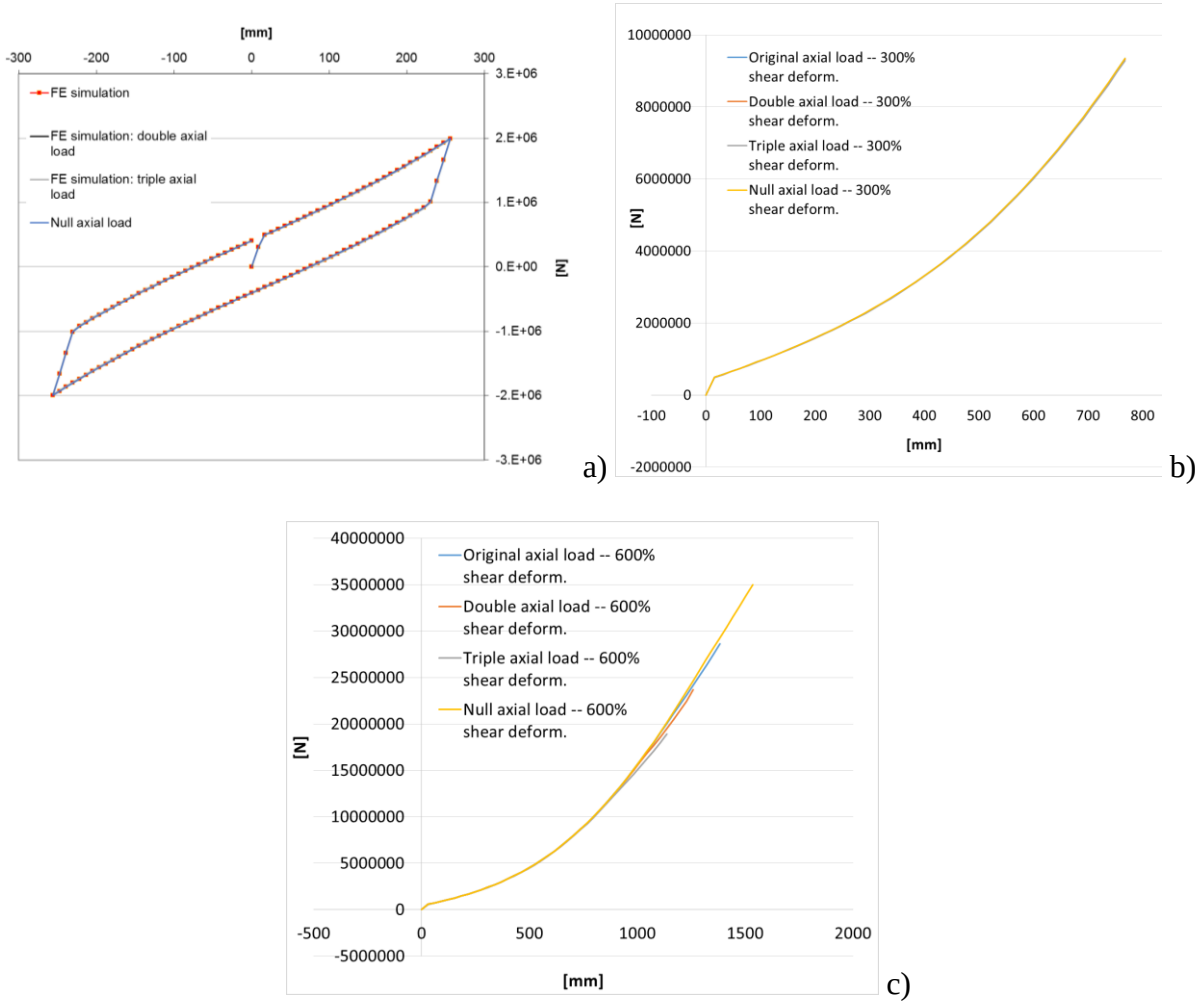

Figure 4. Comparison of FE results: 100% (a), 200% (b), 300% (c) shear loading at different axial forces. Siler isolator.

The curves shown are related to monotonic loading only since we were not able to reproduce the correct dissipation, at this values of shear distortion, either with isotropic and kinematic hardening. Adoption of this type of hardening for reproducing the shape of the hysteresis cycles at larger strain values had to be abandoned due to its poor performances. Also, in literature no references could be found on this topic.
Laboratory experimentations were also focused on the evaluation of the ultimate limit state for de-lamination. In particular a monotonic test up to failure has been performed according to the EN15129:2009 (2009) norm.

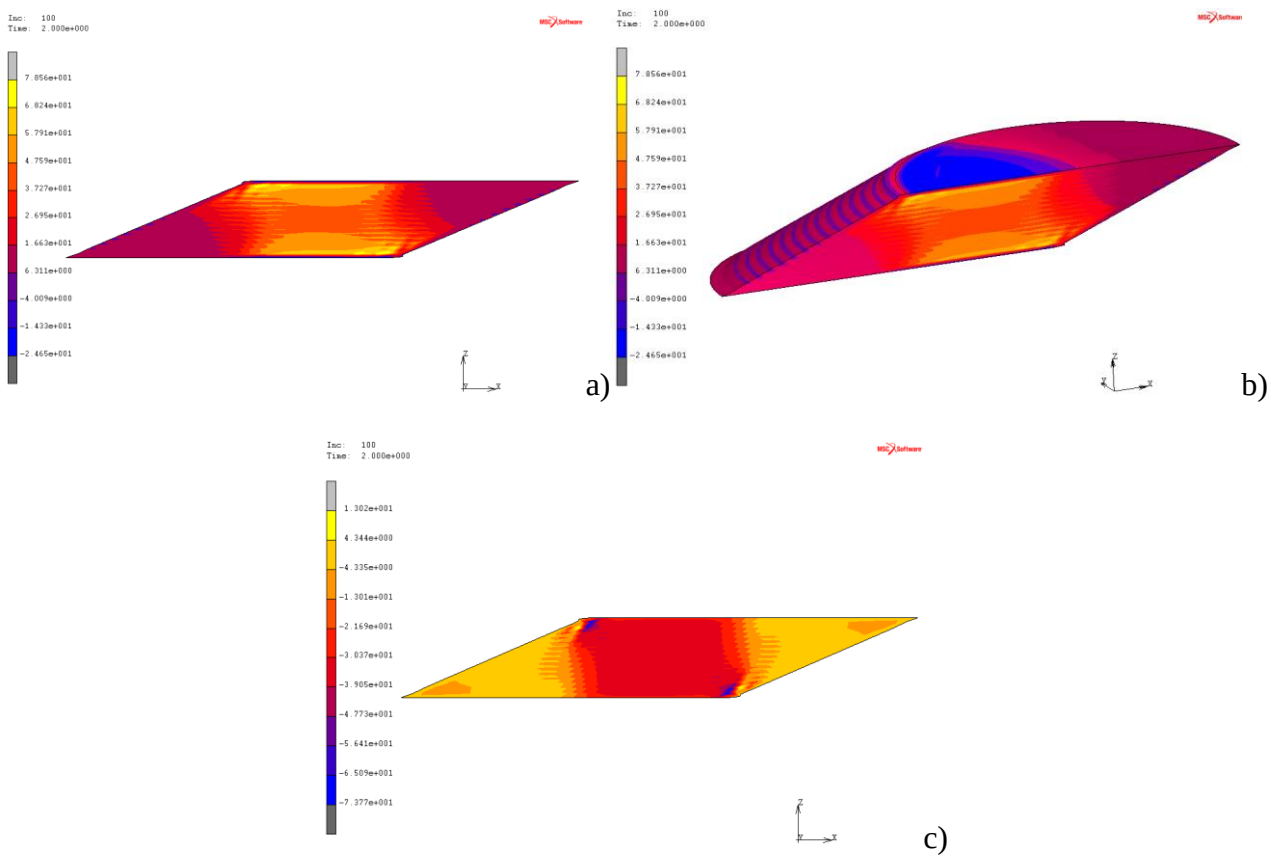

Figure 5. Maximum (a,b) and minimum (c) principal stresses in the numerical model at failure (300% shear deformation, and maximum axial load 24800kN). SILER isolator.

The maximum allowable vertical load and the horizontal displacement at 300% of shear deformation are the ultimate conditions. This same testing condition has been simulated also numerically with the developed isolator model, and the resulting stress state at failure has been depicted in Figures 5a-5c. Figure 5a and 5b report the maximum stresses at failure, while Fig. 5c the minimum ones.

The overlaid FE technique, adopted to model the elastomeric layers, does not easily allow to obtain the resultant stress-field in the rubber volume, due the superposition of two different constitutive models, and the stress value at the delamination limit state had to be computed as the stress at the surface of the steel layers.

4. Scaled devices

Coming to the other two isolator models (namely the ones for device 601 and 302), Figures 6 and 7 report the curves in terms of shear force and horizontal relative displacement. Several values of the axial load have been adopted to assess their influence on the numeric response of devices having different shape, and to provide data for comparison with published results.

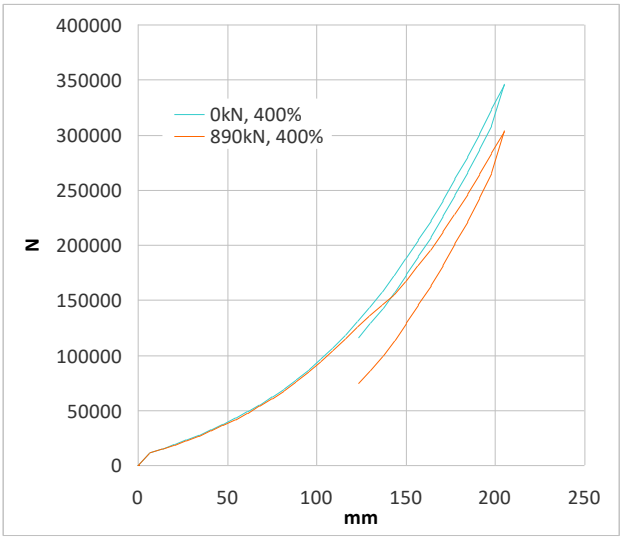

Figure 6. Comparison of FE results: shear loading at different axial forces for device 601 at 400% shear strain.

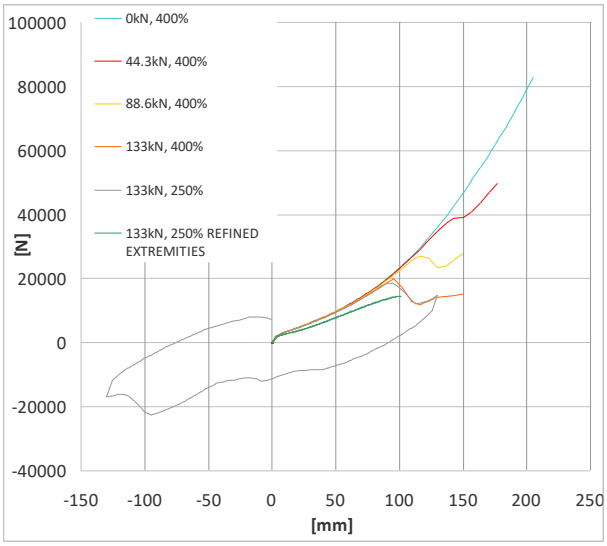

Figure 7. Comparison of FE results: shear loading at different axial forces for device 302 at 400% and 250% shear strain.

Differently from the SILER device, that was really thin and large, the last two show an increasing influence of axial force with the increasing slenderness of the device. Particularly, the most slender device (isolator 302) here considered shows an unstable branch with a critical load that reduces at the in-crease of the axial load. This is consistent with results coming from experiments on devices of similar shape.

The distribution of the internal stresses is also of interest in order to avoid local material or bonding failures. The internal stresses in device 601 are depicted in Figures 8 and 9 while those of device 302 in Figures 10-13. The limit value of 79 MPa for principal maximum stresses, as highlighted from the SILER isolator FE-experimental analysis, is used for establishing the ultimate limit state conditions.

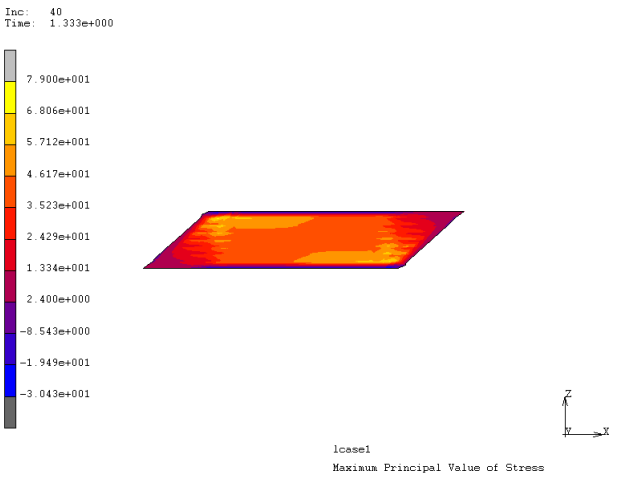

Figure 8. Principal stresses in the numerical model of device 601: axial load 890kN and 140% shear deformation. The maximum principal stresses reach the ultimate value of about 79 MPa.

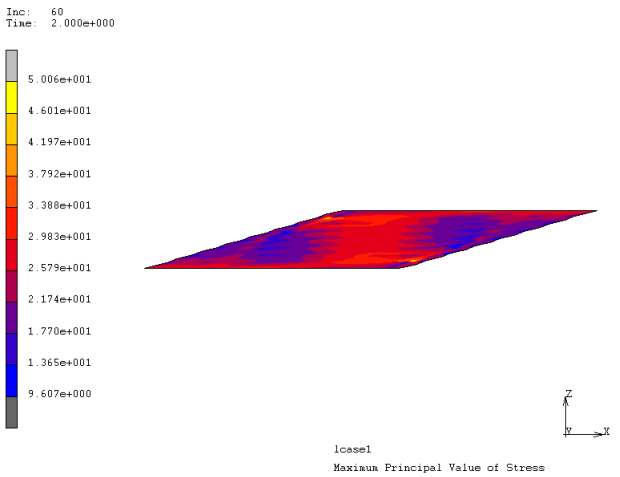

Figure 9. Principal stresses in the numerical model of device 601: zero axial load and 400% shear deformation. The maximum principal stresses stay below the ultimate value of about 79 MPa.

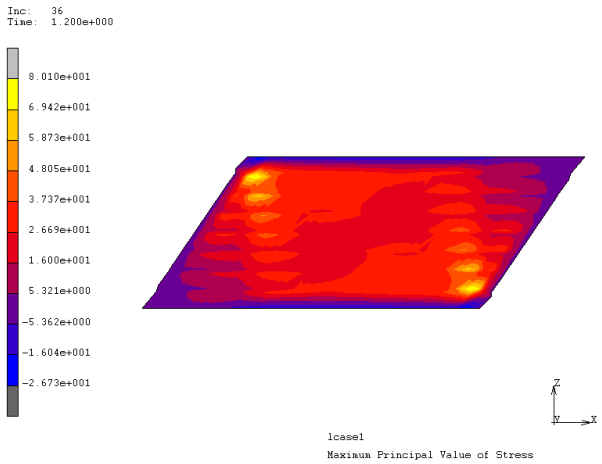

Figure 10. Principal stresses in the numerical model of device 302: axial load 133kN and 85% shear deformation. The maximum principal stresses reach the ultimate value of about 79 MPa.

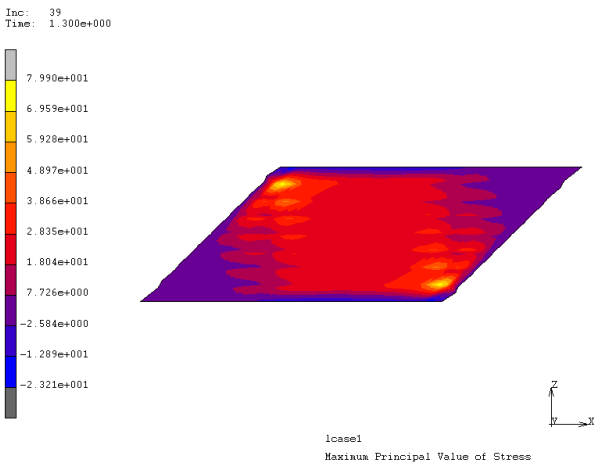

Figure 11. Principal stresses in the numerical model of device 302: axial load 88kN and 130% shear deformation. The maximum principal stresses reach the ultimate value of about 79 MPa.

As these figures show, the experimentally defined limit value of about 79 MPa, that corresponded to debonding in SILER tests of real devices, was reached under a decreasing shear deformation at the increase of the axial load. This is an interesting and significant finding for the design and the implementation of such devices in bridge structures.

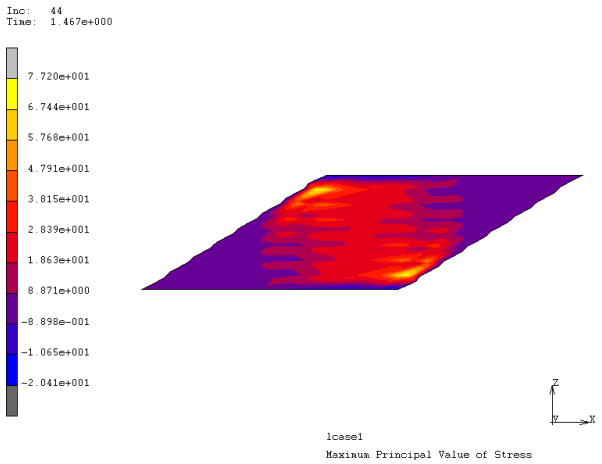

Figure 12. Principal stresses in the numerical model of device 302: axial load 44kN and 200% shear deformation. The maximum principal stresses reach the ultimate value of about 79 MPa.

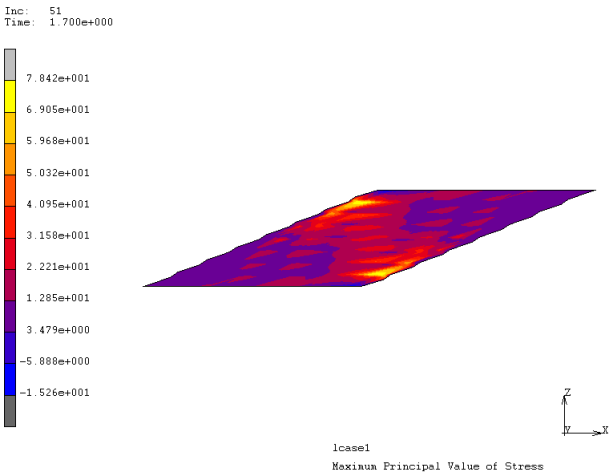

Figure 13. Principal stresses in the numerical model of device 302: zero axial load and 290% shear deformation. The maximum principal stresses reach the ultimate value of about 79 MPa.

5. Conclusions

Scope of the paper is to study the limit state and the beyond design response of filled isolator devices having different aspect ratios. Axial force variability has been deemed as essential for capturing the global response of the base isolation device. Variable axial forces at increasing horizontal displacements have been thus considered in finite element analyses to highlight the dependencies of one on the other. The devices models have been developed adopting the overlapping technique, which allows to predict the hysteretic behaviour of rubber components by a suitable combination of simple constitutive models. The material modes have been tuned on results from tests and laboratory experiments. The elastic-plastic component of the elastomeric layers has

been successfully implemented for the re-production of the device hysteresis at small value of shear deformations. However, this approach was not successful with shear deformations larger than 200%. Further research needs to be devoted to the implementation of special dissipative models, able to capture the physical behaviour of the HDRB at larger values of shear strain. The limit stress state condition of the device has been also assessed. This was carried out by comparing the stress values from the numerical analyses with those derived from laboratory tests at failure. The results pointed out as at the increase of the axial load, the experimentally derived limit value of the principal stresses is reached for a smaller value of the shear deformation.

Acknowledgements

The research leading to these results has received funding from the European Research Council under the Grant Agreement n° ERC_IDEal reSCUE_637842 of the project IDEAL RESCUE— Integrated DEsign and control of Sustainable CommUnities during Emergencies.

References

Basu, B, Bursi, O, Casciati, F, Casciati, S, Del Grosso, A, Domaneschi, M, Faravelli, F, Holnicki, J, Irschik, H, Krommer, M, Lepidi, M, Martelli, A, Oztork, B, Pozo, F, Pujol, G, Rakicevic, Z, Rodellar, J 2014, 'An EACS joint perspective. Recent studies in civil structural control across Europe', *Structural Control & Health Monitoring*, vol. 21 no. 12, pp. 1414–1436.

Bianchi, G, Corradi dell'Acqua, L, Domaneschi, M, Mantegazza, DC, Perotti, F 2011, 'HDRB isolating devices for nuclear power plants: FE modelling and damage/failure characterization', *Structural Engineering World Congress (SEWC2011)*, Cernobbio (CO), Italy.

De Grandis, S, Domaneschi, M, Perotti, F 2009, 'A numerical procedure for computing the fragility of NPP components under random seismic excitation', *Nuclear Engineering and Design*, vol. 239, no.11, pp. 2491-2499.

Domaneschi, M, Martinelli, L, Perotti, F 2012, 'Seismic Rotational Components on Isolated Structures', *Proc. of 15th World Conference on Earthquake Engineering*, Lisbon, Portugal.

Domaneschi, M, Martinelli, L, Perotti, F, Tomasin, M 2015, 'Assessing the performance of a high damping rubber bearing in beyond-design conditions', *Proc. of 10th International Workshop on Structural Health Monitoring, IWSHM 2015*, vol. 2, pp. 1073-1080.

Gracia, LA, Liarte, E, Pelegay, JL, Calvo, B 2010, 'Finite element simulation of the hysteretic behaviour of an industrial rubber. Application to design of rubber components', *Finite Elements in Analysis and Design*, vol. 46, pp. 357-368.

Milani, G, Milani, F 2012, 'Stretch–Stress Behavior of Elastomeric Seismic Isolators with Different Rubber Materials: Numerical Insight', *Journal of Engineering Mechanics*, vol. 138, pp. 416-429.

Nagarajaiah, S, Ferrell, K 1999, 'Stability of elastomeric seismic isolation bearings', *Journal of Structural Engineering*, vol. 125, no. 9, Paper No. 15573.

Perotti, F, Domaneschi, M, De Grandis, S 2013, 'The numerical computation of seismic fragility of base-isolated NPP buildings', *Nuclear Engineering and Design*, vol. 262, no. 189–200.

SILER, European Commission 7th EURATOM Framework Program 2007-2013.

Standard CSN EN 15129 2009. Anti-seismic devices.

Warn, G, Whittaker, A 2008, 'Vertical Earthquake Loads on Seismic Isolation Systems in Bridges', *Journal of Structural Engineering*, vol. 134, no. 11, pp. 1696–1704.